



# Holocene variations of thermocline conditions in the eastern tropical Indian Ocean



Cornelia Kwiatkowski <sup>a,\*</sup>, Matthias Prange <sup>a</sup>, Vidya Varma <sup>a,b</sup>, Stephan Steinke <sup>a</sup>, Dierk Hebbeln <sup>a</sup>, Mahyar Mohtadi <sup>a</sup>

<sup>a</sup> MARUM – Center for Marine Environmental Sciences, University of Bremen, Bremen, Germany

<sup>b</sup> Dept. of Meteorology, Stockholm University, SE-10691 Stockholm, Sweden

## ARTICLE INFO

### Article history:

Received 28 April 2014

Received in revised form

30 November 2014

Accepted 28 January 2015

Available online

### Keywords:

Indian Ocean

Sumatra

Indian Ocean Dipole

Mg/Ca

Thermocline

Holocene

Planktic foraminifera

## ABSTRACT

Climate phenomena like the monsoon system, El Niño Southern Oscillation (ENSO) and the Indian Ocean Dipole (IOD) are interconnected via various feedback mechanisms and control the climate of the Indian Ocean and its surrounding continents on various timescales. The eastern tropical Indian Ocean is a key area for the interplay of these phenomena and for reconstructing their past changes and forcing mechanisms. Here we present records of upper ocean thermal gradient, thermocline temperatures (TT) and relative abundances of planktic foraminifera in core SO 189-39KL taken off western Sumatra (0°47.400' S, 99°54.510' E) for the last 8 ka that we use as proxies for changes in upper ocean structure. The records suggest a deeper thermocline between 8 ka and ca 3 ka compared to the late Holocene. We find a shoaling of the thermocline after 3 ka, most likely indicating an increased occurrence of upwelling during the late Holocene compared to the mid-Holocene which might represent changes in the IOD-like mean state of the Indian Ocean with a more negative IOD-like mean state during the mid-Holocene and a more positive IOD-like mean state during the past 3 ka. This interpretation is supported by a transient Holocene climate model simulation in which an IOD-like mode is identified that involves an insolation-forced long-term trend of increasing anomalous surface easterlies over the equatorial eastern Indian Ocean.

© 2015 Elsevier Ltd. All rights reserved.

## 1. Introduction

Presently, the Indonesian climate is mainly controlled by the seasonal migration of the Intertropical Convergence Zone (ITCZ), the Australian-Indonesian monsoon and the El Niño – Southern Oscillation (ENSO). The Indian Ocean Dipole (IOD) which is a coupled ocean–atmosphere phenomenon also exerts a significant control on the climate variability over western Indonesia (Saji et al., 1999; Webster et al., 1999; Abram et al., 2007). Negative IOD events are characterized by positive rainfall anomalies over western Indonesia accompanied by dry conditions over East Africa and eastward surface wind anomalies over the eastern Indian Ocean. On the other hand a positive IOD event is characterized by sea surface cooling (Fig. 1) and increased productivity off Sumatra due to enhanced upwelling in the eastern Indian Ocean accompanied by strong easterlies over the central Indian Ocean, dry conditions in

West Indonesia and higher-than-normal rainfall over East Africa (Webster et al., 1999).

Behera et al. (2006) suggest that the IOD is initiated by processes internal to the Indian Ocean and, might be additionally affected and amplified by other climatic phenomena as e.g. ENSO. Saji et al. (1999) suggest the IOD being independent of ENSO but model simulations imply that ENSO has a strong influence on the periodicity, strength, and formation processes of the IOD in years of co-occurrences (Behera et al., 2006). However, since the occurrence of three positive IOD events in the years 2006–2008 it is obvious that ENSO is not the only triggering factor (Behera et al., 2006).

Previous studies on the IOD mainly focus on its present-day behavior, but only little is known about its past variability beyond the instrumental record. So far, there exist only three studies from the eastern Indian Ocean investigating the IOD variability during the Holocene; two are based on SST anomaly reconstructions from coralline Sr/Ca ratios off Sumatra (Abram et al., 2007, 2009) and one is based on precipitation changes derived from  $\delta D$  and  $\delta^{13}C$  of plant waxes (Niedermeyer et al., 2014). Two studies investigate the IOD variability in the western Indian Ocean by using a multi-proxy

\* Corresponding author.

E-mail address: [ckwiatkowski@marum.de](mailto:ckwiatkowski@marum.de) (C. Kwiatkowski).

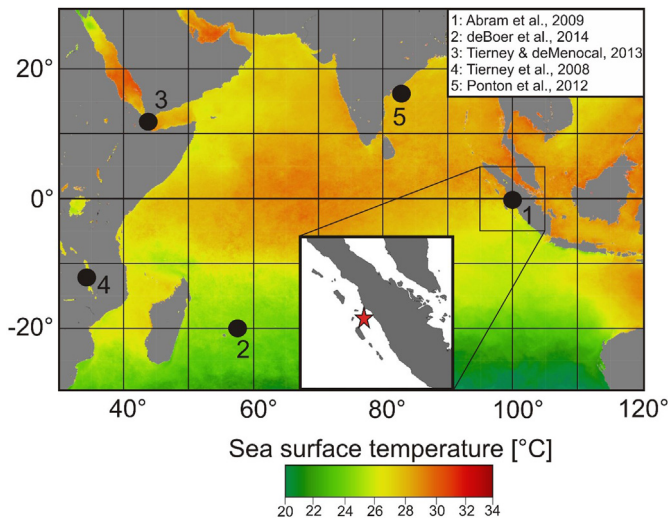


**Fig. 1.** Map of SST in the Indian Ocean indicating the surface cooling caused by the upwelling of cold subsurface water in autumn 2006 during a positive IOD event (<http://oceancolor.gsfc.nasa.gov>). The red star indicates the core site of SO 189-39KL, sites from other studies relevant for this work are numbered serially.

reconstruction from the Mauritian lowlands (de Boer et al., 2014) and  $\delta D$  from Lake Tanganyika sediments (Tierney et al., 2008).

Abram et al. (2007) hypothesize that observed SST anomalies are related to IOD events and suggest the Asian monsoon and ENSO being capable of triggering positive IOD events. They state a close relationship between the Asian monsoon system and IOD implied by a longer duration of positive IOD events during times of strong Asian summer monsoon and argue that sea surface cooling during a positive IOD event is constrained by the cross-equatorial wind reversal at the end of the Asian summer monsoon season resulting in an abrupt termination of Ekman upwelling along the coast of Sumatra (Abram et al., 2007). Furthermore, they assume that the monsoonal wind reversal controlling the timing of peak cooling during positive IOD events to be a consistent feature during the Holocene. The close relationship between the monsoon system and IOD is further supported by the study of Abram et al. (2009). Niedermeyer et al. (2014) investigate regional precipitation patterns over Sumatra in comparison to precipitation patterns from East Africa and Southeast India and find a general agreement with the reconstructed IOD variability by Abram et al. (2009).

The study of de Boer et al. (2014) suggests an anti-phased relationship of climate dynamics between the Mauritian lowlands and western tropical Australia during the middle Holocene reflecting a prolonged configuration of a negative mode of the IOD, which is partly inconsistent with the findings of Abram et al. (2009).

In order to understand the underlying mechanisms and the interaction between the IOD and other climate phenomena, e.g. the monsoon or ENSO continuous long-term data series are essential.

In this study we use a continuous sediment archive recovered from the northern Mentawai Basin off western Sumatra, close to the site published by Abram et al. (2009), in order to estimate variations in upper water column temperature and thermal gradient (i.e. depth of thermocline), and investigate the planktic foraminiferal assemblage to reconstruct the upper water column structure during the past 8 ka. We compare our results to orbital-forced model simulations and other climatic records from the Indian Ocean region in order to better assess possible forcing mechanisms of the upper water column variations off western Sumatra.

## 2. Study area

Aldrian and Susanto (2003) show that under modern conditions, SST and precipitation off western Sumatra are neither controlled by ENSO nor by the monsoonal system but by the seasonal migration of the ITCZ. At present, upper water column temperature and sea surface salinity anomalies in the study area are mainly controlled by the IOD (Yu et al., 2005; Qiu et al., 2012). This is also evident from several SST and TT datasets (e.g. SODA 2.2.4) in comparison to the Dipole Mode Index (DMI) introduced by Saji et al. (1999). Previous studies have shown that the western coast of Sumatra is one of the most sensitive areas for the development of the IOD (e.g. Abram et al., 2007). During positive IOD events, observational data of the last decades have shown that a decrease in SST is accompanied by a decrease in precipitation off Sumatra (Webster et al., 1999). Oceanic thermocline variations associated with IOD are confined to the region north of 6°S (Yu et al., 2005). Large-scale surface and subsurface circulation of the Indian Ocean might not affect the hydrography of the Mentawai Basin due to the topographic situation in which the fore-arc islands impede a direct influence of the open ocean (Mohtadi et al., 2014). Thus, paleo-environmental archives from this area might record changes related to IOD variability. Seasonal changes are weak in the study area (Mohtadi et al., 2014) except for variations related to the IOD, which peaks in the September–October–November (SON) season (Saji et al., 1999). During extreme positive IOD events a SON SST decrease of  $>2$  °C off Sumatra is one of the most significant signals observed presently (Webster et al., 1999; Abram et al., 2007; Du et al., 2008). This surface cooling in the eastern basin of the Indian Ocean is caused by unusually strong upwelling along the equator and off Sumatra. Furthermore, strong precipitation in the eastern Indian Ocean during normal years results in the development of a barrier layer, a layer separating the thermocline and the mixed layer, which impedes the upward movement of subsurface water masses (Spintall and Tomczak, 1992; Du et al., 2005; Qu and Meyers, 2005). During positive IOD events, the reduced warm water advection to the eastern equatorial Indian Ocean (Murtugudde et al., 2000) and the missing barrier layer in the water column due to decreased precipitation allow upwelling of cooler, nutrient-rich subsurface waters to the sea surface (Murtugudde et al., 2000; Du et al., 2008). However, Qiu et al. (2012) and Saji and Yamagata (2003) show that changes in SON SST are relatively small ( $<1$  °C) during most positive IOD events and that temperature changes at the thermocline are much more prominent than changes at the sea surface (cf. Fig. 2). Zhao and Nigam (2015) show that the temperature dipole structure of the IOD occurs at the subsurface whereas the SST field shows a monopole structure over the Indian Ocean. Hence, when using foraminiferal Mg/Ca for the reconstruction of past IOD variations, the depth of thermocline and TT in the eastern Indian Ocean appear to be most suitable to characterize a possible IOD-like mean state – periods characterized either by stronger and/or more frequent positive IOD events (positive IOD-like mean state; upwelling; shallowing of the thermocline) or by weaker and/or less frequent positive IOD events (negative IOD-like mean state; deepening of the thermocline).

## 3. Material and methods

### 3.1. Sample material

Piston core SO189-39KL was recovered from the northern Mentawai Basin off western Sumatra (0°47.400' S, 99°54.510' E, 1350 cm core length, 517 m water depth) during the R/V Sonne 189 – SUMATRA expedition in 2006 (Wiedicke-Hombach et al., 2007; Fig. 1). Here we study the upper 2.7 m of this core representing the

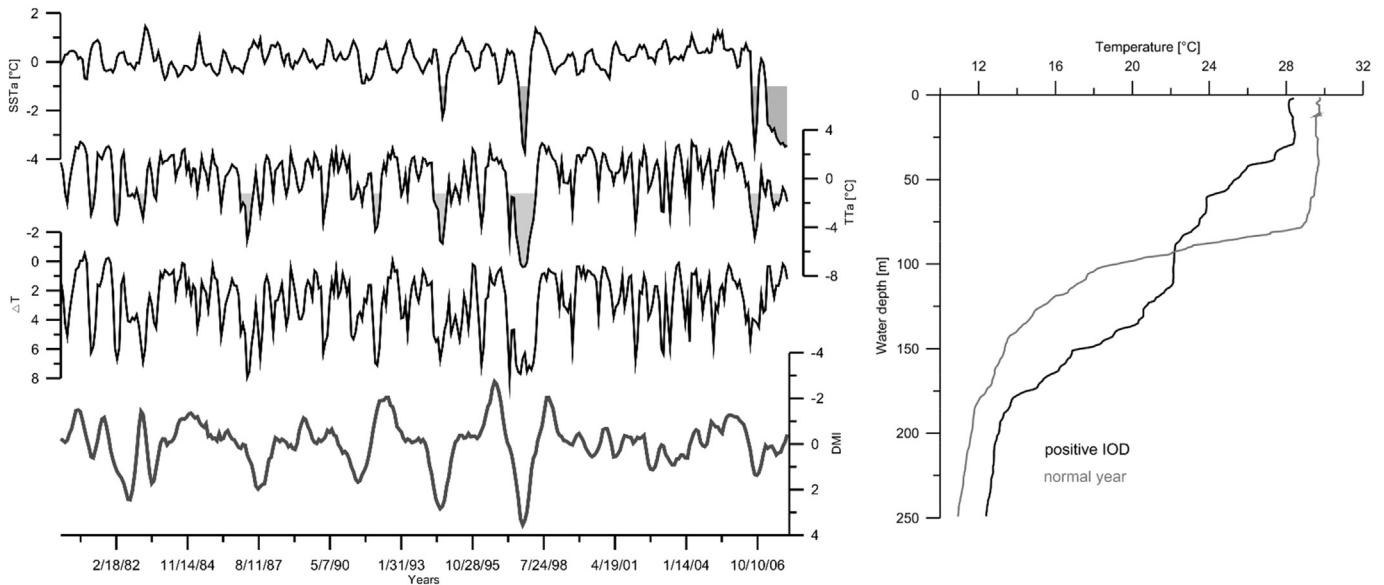


**Fig. 2.** Monthly SST (5 m) and TT (70 m) anomalies relative to the mean SST and TT during Jan. 1980 to Dec. 2007 and  $\Delta T_{\text{SST-TT}}$  calculated from SODA 2.2.4 time series from 0.75S 99.75E (<http://iridl.ldeo.columbia.edu>; Carton et al., 2005) during the years 1980–2007 compared to the Dipole Mode Index (Saji et al., 1999). The gray filling in the SST and TT records indicate anomalies exceeding the error of 1 °C for SST and 1.2 °C for TT reconstructions, respectively. Additionally, a comparison of water temperature profiles measured during August 2005 (normal year, Mohtadi et al., 2007) and September 2006 (positive IOD year, Mohtadi et al., 2007) in the Mentawai Basin indicates an uplift of the thermocline and a SST cooling of 1 °C during a positive IOD event.

past 8000 years. The continuous occurrence of pteropods throughout the core implies good preservation of carbonate. The age model for this period is based on 20 AMS radiocarbon dates (Mohtadi et al., 2014).

### 3.2. Planktic foraminiferal trace element analysis

SST anomaly (a), T<sub>Ta</sub> and,  $\Delta T$  between 1980 and 2007 calculated from the SODA 2.2.4 dataset in comparison to the Dipole Mode Index (DMI) introduced by Saji et al. (1999) illustrate the relationship of upper water column characteristics to the IOD (Fig. 2). SODA 2.2.4 dataset represents realistic changes in timing and magnitude of SST variations therefore changes of TT might be also reliable. Large variations, especially in TT, correspond to variations in the IOD (correlation coefficient of  $-0.52$  between T<sub>Ta</sub> and DMI and  $0.43$  between  $\Delta T$  and DMI; Fig. 2), thus, highlighting the suitability of TT off western Sumatra as a proxy to track past IOD changes.

The core was sampled at 2 cm intervals (sample resolution of ~60 years) for trace element analyses on thermocline dwelling planktic foraminifera *Pulleniatina obliquiloculata* with a calcification depth of ~75 m (Mohtadi et al., 2011a). Due to weak seasonal changes in the study area, we suggest an annual occurrence of *P. obliquiloculata*. Since upwelling and hence substantial shifts in thermocline depth can only occur during the IOD peak season, variations in the thermocline record should mainly reflect changes in the SON season.

For Mg/Ca analyses ~25 individuals of *P. obliquiloculata* from the size-fraction 355–500  $\mu\text{m}$  were picked. For the selected foraminifera we applied the cleaning protocol originally proposed by Barker et al. (2003) consisting of a clay-removal step using ultra-pure water and methanol, followed by the oxidation of organic matter using 1% NaOH-buffered H<sub>2</sub>O<sub>2</sub>. The samples were dissolved into 0.075 M QD HNO<sub>3</sub> and centrifuged for 10 min at 6000 rpm. The solution was transferred into test tubes and diluted to the final volume dependent on the amount of calcite contained in each sample. The trace element concentrations were measured with Inductively Coupled Plasma Optical Emission Spectrometry

(Agilent Technologies 700 Series ICP-OES & Cetac ASX-520 auto-sampler) by using a multi-element approach at the MARUM, University of Bremen. The Mg/Ca values are reported as mmol mol<sup>-1</sup>. The instrumental precision of the measurements was monitored by using an external standard solution (Mg/Ca = 2.97 mmol mol<sup>-1</sup>) measured after every fifth sample as well as the ECRM 752-1 standard measured after every 50 sample, providing a standard deviation of 0.005 mmol mol<sup>-1</sup> (0.17%) for the external standard and 0.002 mmol mol<sup>-1</sup> (0.06%) for the ECRM 752-1 standard, respectively. The reproducibility of the samples was 6.9% (n = 10) corresponding to a standard deviation of 0.2 mmol mol<sup>-1</sup> (Fig. 3b, error bar). Aluminum, which usually indicates a contamination by silicate minerals (Barker et al., 2003), is under the detection limit. Post-depositional Mn-rich carbonate/oxyhydroxides coatings can bias foraminiferal Mg/Ca ratios (Pena et al., 2005), and can be detected by foraminiferal Fe/Ca and Mn/Ca ratios. Due to relatively high Fe/Ca and Mn/Ca ratios, the influence of contaminant phases on Mg/Ca temperature estimates was determined via cross plots. No covariance between Mn/Ca and Mg/Ca ratios ( $r^2 = 0.02$ ) or between Fe/Ca and Mg/Ca ratios ( $r^2 = 0.11$ ) could be observed. Consequently, we infer the Mg/Ca values of the Holocene section of SO 189-39 KL to be unaffected by contaminant phases.

*P. obliquiloculata* Mg/Ca ratios were converted into temperatures (T) using the species specific equation proposed by Anand et al. (2003):

$$\text{Mg/Ca}_{P. obliquiloculata} = 0.328 \exp(0.09T)$$

The error of the temperature reconstructions based on *P. obliquiloculata* Mg/Ca is estimated by propagating the errors introduced by the Mg/Ca measurements and Mg/Ca-temperature calibration (see Mohtadi et al., 2014 for details). The resulting error is on average 1.2 °C (Fig. 3c). The upper water vertical temperature gradient ( $\Delta T$  °C) has been estimated by subtracting thermocline temperatures (TT, based on Mg/Ca<sub>*P. obliquiloculata*</sub>) from SST (based on Mg/Ca<sub>*G. ruber s.s.*</sub>, published in Mohtadi et al., 2014). *Globigerinoides ruber s.s.* has a calcification depth of 0–30 m

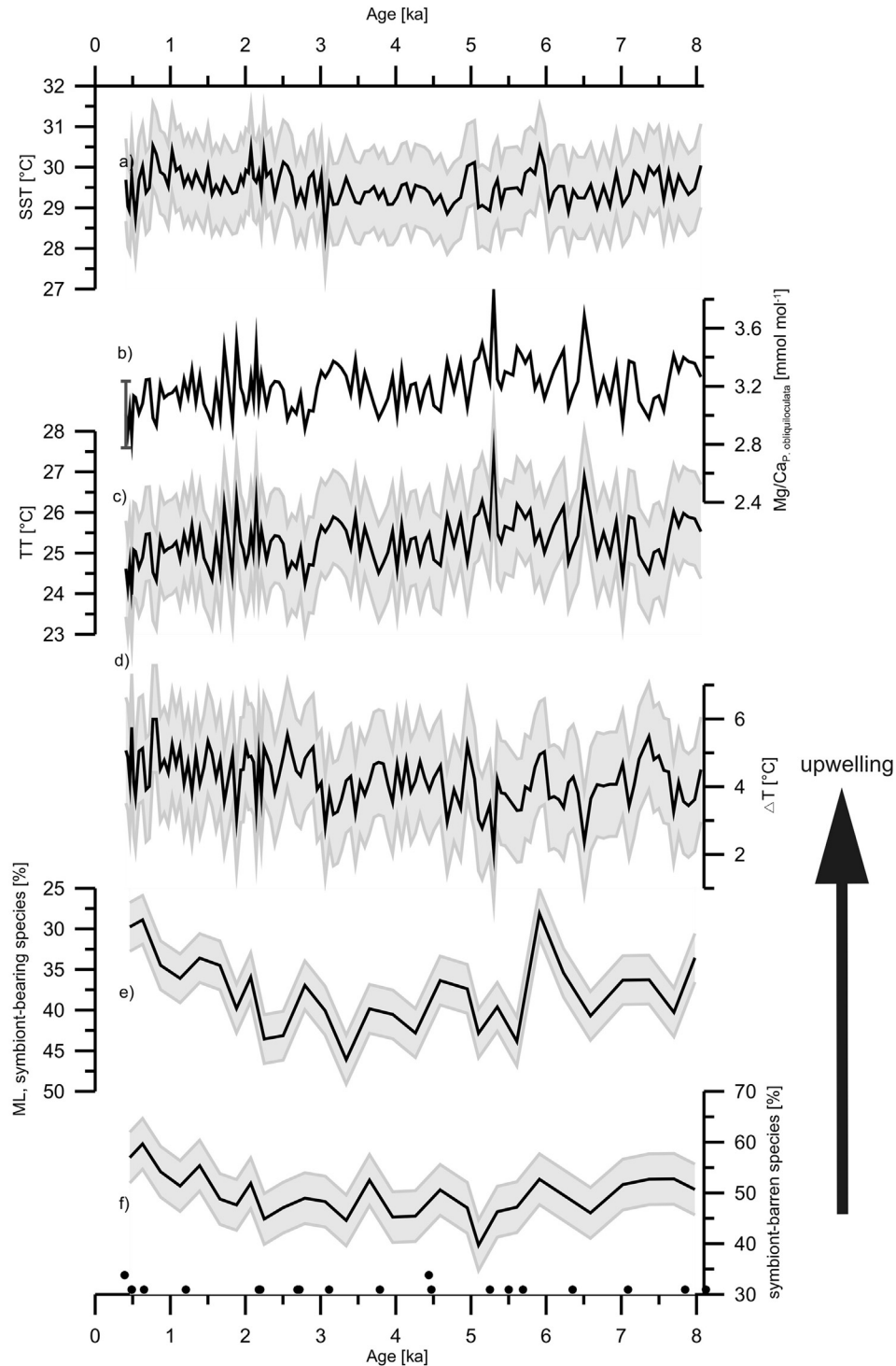


**Fig. 3.** Analytical results of SO 189-39KL: a) SST estimates derived from Mg/Ca ratios of *G. ruber* s.s. (Mohtadi et al., 2014), b) Mg/Ca ratios of *P. obliquiloculata*, c) TT estimates derived from Mg/Ca ratios of *P. obliquiloculata*, d) temperature difference between SST and TT, e) abundance of planktic, ML dwelling, symbiont-bearing foraminifera and AMS  $^{14}\text{C}$  dates (dots; Mohtadi et al., 2014).

(Mohtadi et al., 2011a). The error of the  $\Delta T$  ( $^{\circ}\text{C}$ ) estimates was calculated by using the errors of the SST and TT ( $\pm 1.6^{\circ}\text{C}$ , Fig. 3d). A smaller difference in  $\Delta T$  indicates a lower temperature gradient and hence a deeper thermocline. A greater difference in  $\Delta T$  indicates a larger temperature gradient and consequently, a shoaling of the thermocline typical for upwelling conditions (Mohtadi et al., 2010; Steinke et al., 2011).

### 3.3. Planktic foraminiferal assemblage

At every 10 cm a minimum of 300 individuals of planktic foraminifera from the size fraction  $>125\ \mu\text{m}$  were counted. The abundance of single species relative to total planktic foraminifera was calculated. The abundance of mixed-layer (ML) dwelling, symbiont-bearing foraminifera and ML and thermocline dwelling, symbiont-

barren foraminifera was used to assess the nutrient availability related to upwelling conditions in the study area. ML dwelling, symbiont-bearing foraminifera are able to cope with the disadvantages of a deep mixed layer (e.g. during a more negative IOD-like mean state), while ML and thermocline dwelling, symbiont-barren foraminifera prefer nutrient-rich waters (e.g. during a positive IOD-like mean state). To obtain the statistical error the standard deviation was calculated on 3 replicate counts of 3 replicate splits, respectively. The counts have a relative error of 3% for ML dwelling, symbiont bearing foraminifera (*Orbulina universa*, *Globigerinoides conglobatus*, *G. ruber*, *Globigerinoides sacculifer*, *Globigerina aequilateralis*, *Globigerina falconensis*) and 5% for ML and thermocline dwelling, symbiont-barren foraminifera (*Globigerina bulloides*, *Neogloboquadrina dutertrei*, *Neogloboquadrina pachyderma*, *Pulleniatina obliquiloculata*, *Globigerina glutinata*, *Globigerina calida*, *Globorotalia scitula*, *Globigerina quinqueloba*, *Globorotalia tumida*).

### 3.4. Climate modeling

Output from transient Holocene climate simulations (Varma et al., 2012) was analyzed to help interpreting the proxy records. The simulations were performed using the low-resolution (T31 or 3.75° atmosphere) version of the comprehensive climate model CCSM3 (Yeager et al., 2006), which is a fully-coupled atmosphere-ocean general circulation model (Collins et al., 2006). From a pre-industrial equilibrium simulation, the model was integrated for 400 years with conditions representing 9 ka orbital forcing to reach a new quasi-equilibrium. After this spin-up, three transient Holocene (9–0 ka) simulations, which differ in their initial conditions, were carried out, where orbital forcing has been accelerated by a factor 10 (cf. Lorenz and Lohmann, 2004). While the first transient run was initialized with the quasi-equilibrated 9 ka state, the second and third runs used the 8.9 and 8.8 ka climates from the first transient run as initial conditions at 9 ka. Greenhouse gas concentrations, aerosol and ozone distributions have been kept constant at pre-industrial values in all Holocene experiments. Moreover, modern continental ice sheets were prescribed such that variations in the orbital parameters were the sole external forcing in the transient runs. The reader is referred to Varma et al. (2012) for a detailed description of the model setup and experimental design.

Spatio-temporal patterns of low-level (850 hPa) zonal wind variability over the Indian Ocean were examined by means of empirical orthogonal function (EOF) analysis using the three-member ensemble average (averaging over the different runs reduces the influence of stochastic internal climate variability on the results). The EOFs (or principal components) were found by computing the eigenvalues and eigenvectors of the wind-field covariance matrix (e.g. von Storch and Zwiers, 2004). The derived eigenvalues provide a measure of the percent variance explained by each mode (the first or leading mode provides the highest variance in the wind field). The time series of each mode were obtained by projecting the derived eigenvectors onto the spatially weighted anomalies.

## 4. Results

### 4.1. Mg/Ca Paleothermometry, upper water column structure and faunal analysis

The TT estimates fluctuate between 24 and 27.5 °C (2.8 and 3.8 mmol mol<sup>-1</sup>) and are in good agreement with the SODA 2.2.4 dataset but also the CTD profiles which show a temperature at 70 m water depth of 23–24 °C during positive IOD events and 27–29 °C

during normal years (Fig. 2). TT estimates show a strong variability and discernable long-term variations with a general increase observable during the early Holocene, which peaks during the mid-Holocene (~26 °C at about 5 ka) and decreases thereafter towards the present (~24 °C, Fig. 3b, c). The SST estimates remain relatively constant during the Holocene (Fig. 3a, Mohtadi et al., 2014) and vary between 28.3 and 30.5 °C (4.9 and 5.9 mmol mol<sup>-1</sup>). They show a slight decreasing trend between 8 and 6 ka followed by a period of strong SST fluctuations between 6 and 5.5 ka and a cooler and more stable period between 5.5 and 2.5 ka. The late Holocene is characterized by large variations and relatively high SST (~29.7 °C), interrupted by a period of slightly cooler SST between 1.9 and 1.2 ka.

Strong fluctuations in  $\Delta T$  can be recognized throughout the Holocene with values ranging between 2 and 6 °C (Fig. 3d). The early to mid-Holocene is characterized by a lower  $\Delta T$  (4 ± 0.7 °C). At around 3 ka, a shift from lower to higher values takes place, and  $\Delta T$  remains high towards the present (4.6 ± 0.6 °C). This difference is highly significant (p < 0.01) according to the t-test. A decrease from 40% to 30% in the abundance of ML dwelling, symbiont-bearing foraminifera coincides with an increase from 50% to 60% in the abundance of ML and thermocline dwelling, symbiont-barren foraminifera during the late Holocene (Fig. 3e, f). Power spectra (95% significance level) of SST, TT and  $\Delta T$  indicate cycles centered at ~3850, ~1540 and ~1290 years for SST, ~3850, ~2570, ~1100, ~150 years for TT and, ~1540 and ~150 years for  $\Delta T$ .

### 4.2. Model results

The leading EOF of the annual mean zonal wind field (three-member ensemble average; see above) explains 23% of the variance and contains the long-term Holocene trend. It shows a continuous increase of surface westerlies over the equatorial Indian Ocean and Southeast Asia (Fig. 4, upper panel; reddish region because the principal component time series has a negative trend) which is associated with the weakening of the Indian monsoon. The first EOF of the SON season (24% variance explained) shows an almost similar pattern over the West Pacific/Philippines region (Fig. 4, lower panel; bluish region because the corresponding principal component time series has a positive trend). By contrast, an opposite trend is simulated over the tropical eastern Indian Ocean/Indonesian region with increasing easterly surface wind anomalies (reddish region). We note that qualitatively the same EOF patterns and time series were reproduced in all three individual Holocene runs.

## 5. Discussion

Our  $\Delta T$  show a shift from lower to higher values at around 3 ka, indicating a shoaling of the thermocline off western Sumatra during the late Holocene. This is supported by the decrease in the relative abundance of ML dwelling, symbiont-bearing planktic foraminifera and an increase in ML and thermocline dwelling, symbiont-barren planktic foraminifera indicating a shift to an intensified upwelling (Fig. 3e, f). We suggest that changes in the IOD-like mean state might control the long-term variations in TT and  $\Delta T$ . We interpret warmer TT and a smaller  $\Delta T$  between 8 and 3 ka to reflect a more negative IOD-like mean state, whereas colder TT estimates and a greater  $\Delta T$  after 3 ka are interpreted to reflect a more positive IOD-like mean state. Reconstructed Holocene TT variations are relatively small compared to the TT changes of the past three decades as indicated by the CTD or SODA 2.2.4 data at the calcification depth of *P. obliquiloculata* (~6 °C, Fig. 2). We attribute this discrepancy to a smoothing of the IOD-related temperature anomalies in our samples that encompass different seasons and several years.

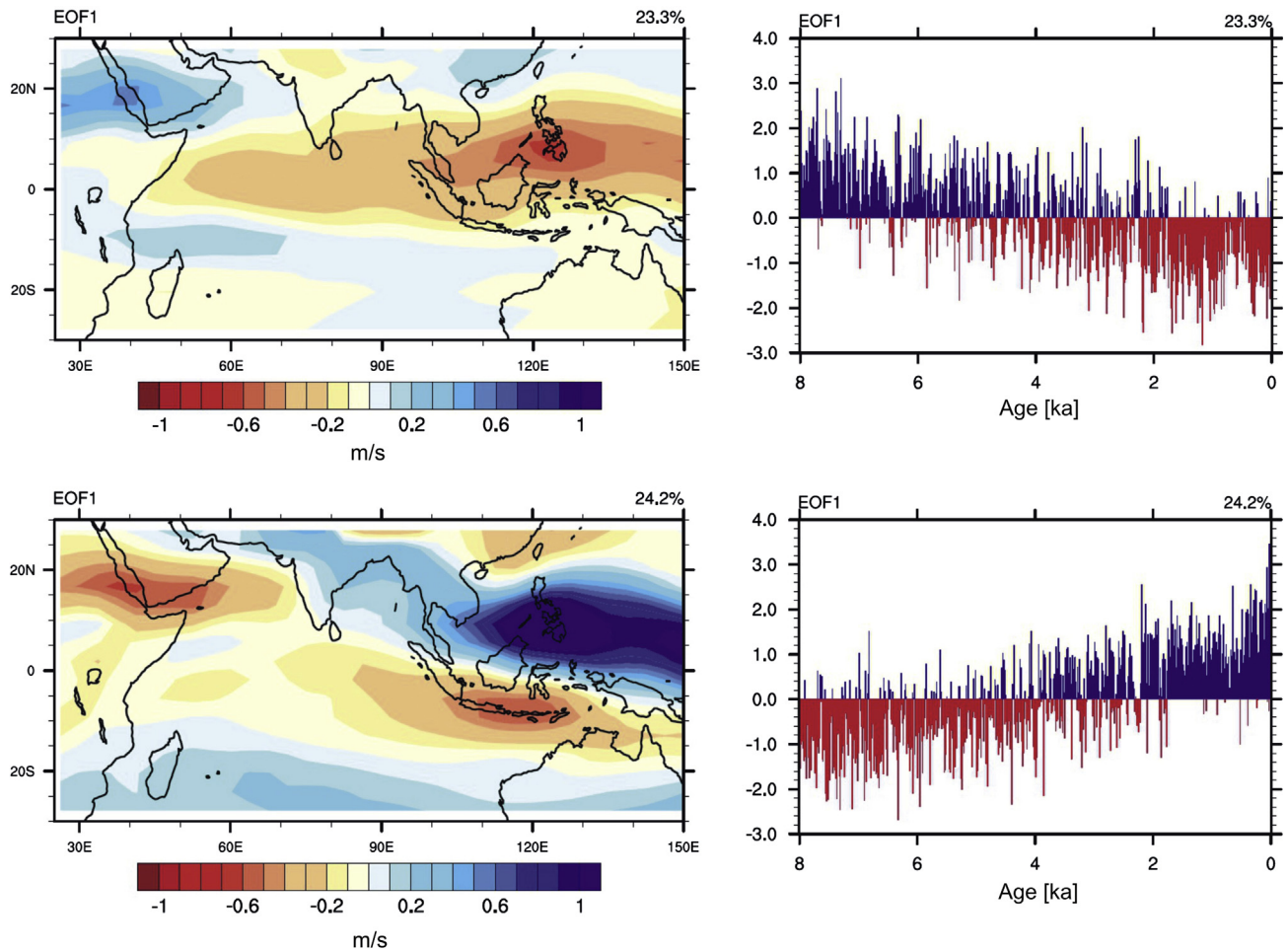


**Fig. 4.** The spatial distribution and time-series of the first empirical orthogonal function (EOF) of annual-mean (top) and September–October–November (bottom) 850 hPa zonal wind simulated for the period 8 to 0 ka by CCSM3 using orbital acceleration with a factor of 10. The EOF analysis was performed on a three-member ensemble mean. The time-series are standardized and the EOF maps are obtained by regressing the wind data onto the corresponding standardized leading principal component time-series. Positive (negative) values in the maps correspond to westerly (easterly) wind anomalies. Multiplication of the values with the time-series provides the Holocene trends.

Abram et al. (2007, 2009) observe a SST cooling of  $>2\text{ }^{\circ}\text{C}$  off Sumatra during the 1997 positive IOD event. Saji and Yamagata (2003) and Qiu et al. (2012) show only a moderate SST cooling of  $<1\text{ }^{\circ}\text{C}$  during most of the 20th century positive IOD events. Deshpande et al. (2014) propose a difference between strong and weak positive IOD events: Strong IOD events driven by a thermocline–SST coupling are strongly interactive with the atmosphere, whereas weak IOD events are a response to surface winds without such dynamical coupling. The thermocline–SST coupling is primarily responsible for the enhanced SST gradient during strong IOD years leading to an anomalous Walker circulation within the Indian Ocean. Therefore, weaker positive IOD events have a weaker effect on SST in the eastern Indian Ocean than strong positive IOD events. Due to an error of  $\sim 1\text{ }^{\circ}\text{C}$  in our foraminiferal SST reconstruction, a more robust signal is expected from reconstructed variations in thermocline temperatures and upper water column structure. Moreover, in-situ observations indicate only a SST cooling of  $\sim 1\text{ }^{\circ}\text{C}$  between a normal year (August 2005) and a positive IOD year (September 2006), but a significant shoaling of the thermocline during the positive IOD year in comparison to the normal year (Fig. 2, Mohtadi et al., 2007). This is corroborated by the comparison of the SODA 2.2.4 time series to the DMI (Fig. 2), further supporting the feasibility of using thermocline conditions as a sensitive proxy for IOD reconstructions. We therefore suggest that our approach of reconstructing the IOD-like mean state of the Indian Ocean during

the Holocene is only capable of discriminating between periods characterized by more frequent and stronger positive or negative IOD events.

Our interpretation of the proxy data is corroborated by the results of the transient Holocene climate model simulation. The first EOF of the SON season shows an IOD-like pattern (cf. Saji et al., 1999; Qiu et al., 2012) with an increasing trend of surface easterly wind anomalies over the equatorial eastern Indian Ocean and Indonesian region, indicating a trend towards more positive IOD-like conditions during the late Holocene (Fig. 4). These anomalous easterly winds induce a shoaling of the tropical thermocline in the eastern Indian Ocean. The simulated interannual zonal surface wind and  $\Delta T$  (temperature difference between surface and thermocline at 70 m depth) variations off the equatorial Sumatran coast are highly correlated for the SON season with  $r = -0.71$  at a model grid point nearest to the core location.

The reconstructions of Abram et al. (2009) show periods of a more positive IOD-like mean state e.g. during the mid-Holocene and periods of a more negative IOD-like mean state e.g. during the late Holocene and are partly anti-correlated to our  $\Delta T$  record (Fig. 5b, c). This might be attributed to the different sample resolutions used in both studies: the reconstructions using corals allow the detection of single IOD events while our sedimentary record only allows the detection of long-term variability in the IOD-like mean states due to the general lower resolution of sedimentary

archives. Considering that SST estimates derived from *G. ruber* are used to calculate  $\Delta T$ , reconstructed upwelling intensity based on  $\Delta T$  tends to be overestimated. *G. ruber* as a warm water species does not favor upwelling conditions and therefore might record annual mean temperatures with a stronger emphasis on non-upwelling seasons.

At present, another characteristic feature of the IOD is the contrasting rainfall pattern over the eastern and the western Indian Ocean. Sea surface salinity reconstructions shift from fresher to saltier conditions around  $\sim 3$  ka as deduced from  $\delta^{18}\text{O}_{\text{sw}}$  reconstructions (Fig. 5a, Mohtadi et al., 2014). However, the observed variations in  $\delta^{18}\text{O}_{\text{sw}}$  are only minor and might not be a reliable indicator for precipitation changes during the Holocene. Rainfall reconstruction of western Sumatra based on  $\delta\text{D}$  of plant waxes show two distinct periods of enhanced precipitation and a supposedly more negative IOD-like mean state between 6.5 and 8 ka and between 1 and 2 ka (Fig. 5d, Niedermeyer et al., 2014). This is partly in contrast to our reconstruction as well as to the reconstructions of Abram et al. (2009). Niedermeyer et al. (2014) suggest that the mid-Holocene decrease in precipitation off western Sumatra coeval with a decrease in East African rainfall and a warm SST anomaly off Sumatra (Abram et al., 2009) might be a result of a non-linear relationship between the eastern Indian Ocean SST and western Indian Ocean rainfall pattern. Alternatively, they argue that the core site of SO189-144KL might not be located within the center of precipitation changes during that time. Additional precipitation data from western Sumatra is necessary in order to better evaluate the IOD induced rainfall changes in the eastern Indian Ocean.

Tierney et al. (2013) reconstruct variations in precipitation over the western Indian Ocean on decadal timescales. Compared to Makassar Strait SST, this gives evidence that East African rainfall might be controlled by the Walker circulation over the Indian Ocean. Tierney et al. (2008) analyze the  $\delta\text{D}$  of leaf waxes from Lake Tanganyika, which indicates a major shift to dry conditions around 4.7 ka (Fig. 5g) consistent with lake level reconstructions from Lake Turkana showing a water-level drop of  $\sim 50$  m around 5.3 ka (Garcin et al., 2012). This is supported by the study of Tierney and deMenocal (2013) using  $\delta\text{D}$  of leaf waxes from a marine record in the Gulf of Aden (Fig. 5f). Comparison with other hydroclimate reconstructions shows a coherent picture of the development of the African Humid Period over northeast Africa, and suggests that the hydroclimate is mainly controlled by the African monsoonal system (Tierney and deMenocal, 2013). In comparison to our proxy data no correlation of climatic shifts can be identified and therefore we assume that the long-term IOD-like mean state signal is too weak in the western Indian Ocean. The IOD signal might be masked by the strong monsoon signal in the Holocene climate records from East Africa and the western Indian Ocean (de Boer et al., 2014) which further complicates a straightforward comparison of the eastern and the western Indian Ocean climate archives. This assumption is further supported by coherent changes in reconstructed Holocene SST anomalies off Tanzania (Kuhnert et al., 2014) and rainfall anomalies in Flores, Indonesia (Griffiths et al., 2009), with positive SST anomalies off East Africa corresponding to positive rainfall anomalies over South Indonesia and vice versa. Kuhnert et al. (2014) therefore suggest that mid-Holocene climate was anomalous on a global scale and hypothesize that the unusual temperature pattern in the Indian Ocean reflects remote forcing rather than one of the climate modes internal to the Indian Ocean. Proxy-based reconstructions, including this study, might also incorporate other seasons and years which would hamper a direct comparison additionally.

Swapna and Krishnan (2008) suggest a strong pressure gradient along the equator producing an eastward equatorial undercurrent

that leads to upwelling of cold subsurface waters in the eastern Indian Ocean during times of strong summer monsoon. During a weak summer monsoon, this pressure gradient is too weak to create an equatorial undercurrent and the resulting upward movement of subsurface waters in the eastern Indian Ocean (Swapna and Krishnan, 2008). This IOD-monsoon coupling has also been suggested for the past, with longer and stronger positive IOD events during the monsoon-dominated mid-Holocene (Abram et al., 2007). However, more positive IOD events during the last decades (Abram et al., 2008; Ihara et al., 2008; Cai et al., 2009) are associated with a weakening of the Indian summer monsoon (Naidu et al., 2009; Cai et al., 2013). Thus, observations suggest that both the sign and the phase of the IOD-monsoon relationship can change over decades, and it is likely that such changes also occurred in the past. Li et al. (2003) suggest a negative feedback mechanism between the Indian summer monsoon and the IOD leading to a contemporaneous decrease in precipitation over India and Indonesia. A positive IOD might strengthen the Indian monsoon whereas a strengthened Indian monsoon might weaken the IOD (Li et al., 2003). This relationship is also evident from our reconstruction when a positive IOD-like mean state during the late Holocene corresponds to a period of weaker Asian summer monsoon (Wang et al., 2005; Fleitmann et al., 2007; Mohtadi et al., 2011b), whereas a more negative IOD-like mean state during the mid-Holocene is accompanied by a stronger Asian summer monsoon (Wang et al., 2005; Fleitmann et al., 2007; Mohtadi et al., 2011b). Spectral analyses of our records from the eastern tropical Indian Ocean indicate an influence of solar activity with cycles of 2500, 1000 and, 150 years (Debret et al., 2007; Abreu et al., 2012) together with a 1.5 ka cyclicity that might reflect the Bond cycles in the North Atlantic (Bond et al., 2001). It is suggested by previous studies that solar activity has a significant influence on monsoonal precipitation indicated by cycles centered at  $\sim 150$  years (Fleitmann et al., 2003; Wang et al., 2005). However, due to the relatively low temporal resolution of our records interpretations on a monsoon-IOD relationship on these frequencies would be speculative. Abram et al. (2007) propose a close relationship between the monsoonal system and the IOD because the monsoonal wind reversal at the onset of the NW monsoon terminates IOD events. However, IOD events also have a prominent influence on the moisture transport by monsoonal surface winds into areas surrounding the Indian Ocean. During the positive IOD event in 1994, when a positive IOD and an El Niño event co-occurred (Ding and Li, 2012), an enhanced convection over India resulted in heavy precipitation over Northern India, the Bay of Bengal, Indochina and Southern China (Behera et al., 1999; Guan and Yamagata, 2003). Large anomalies in Indian summer monsoon rainfall can be related to an additive influence of ENSO and the equatorial Indian Ocean Oscillation, the atmospheric component of the IOD (Gadgil et al., 2004) or strong IOD events (Deshpande et al., 2014). While during El Niño events an anomalous divergence over India cause anomalous subsidence and weakens the Indian summer monsoon rainfall, positive IOD-induced wind anomalies weaken the influence of ENSO and persuade a convergence over the Indian monsoon region (Ashok et al., 2004). Ponton et al. (2012) reconstruct the Holocene monsoon variability by using carbon isotopes of sedimentary leaf waxes in a marine record in the Bay of Bengal off the Godavari River. This record reflects a gradual increase in aridity-adapted flora indicating a decrease in precipitation during the Holocene (Fig. 5e). Climatic conditions in India became drier during the late Holocene whereas our  $\Delta T$  reflects a more positive IOD-like mean state (Fig. 5b). The orbitally-forced weakening of the monsoon during the Holocene might have led to a shift to a more positive IOD-like mean state of the Indian Ocean, amplified by more frequent and intensive El Niño events (Li et al., 2003).

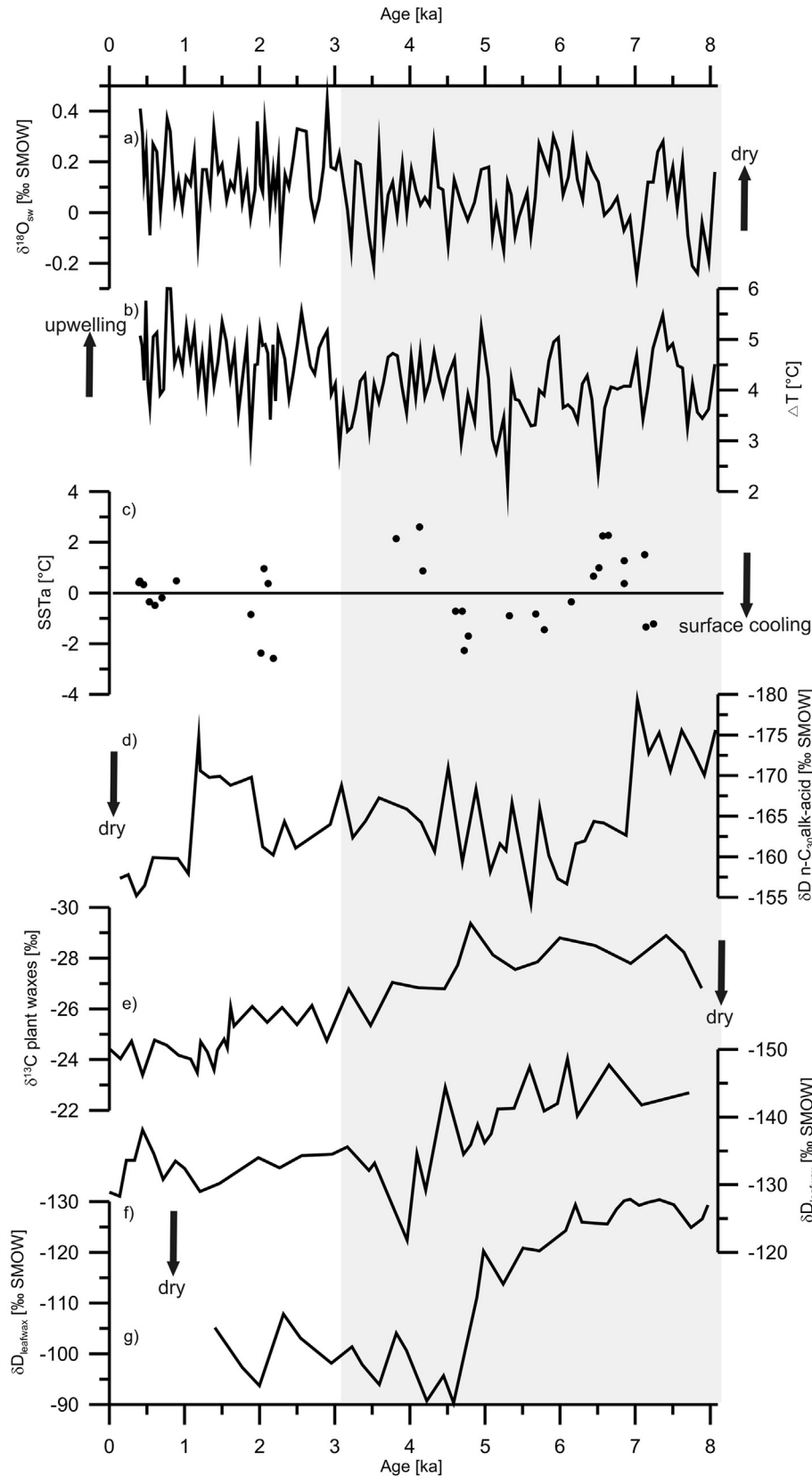


**Fig. 5.** Comparison of a)  $\delta^{18}\text{O}_{\text{sw}}$  indicating variations in sea surface salinity (Mohtadi et al., 2014), b)  $\Delta T$  derived from SST estimates – TT estimates indicating the mixed layer thickness, c) coralline SST anomaly reconstructions (Abram et al., 2009), d)  $\delta D$  from SO189-144KL indicating rainfall variations off West Sumatra (Niedermeyer et al., 2014), e)  $\delta^{13}\text{C}$  from plant waxes from India indicating an aridification in India during the Holocene (Ponton et al., 2012), f)  $\delta D$  from leaf waxes from marine record P178-15P from the Gulf of Aden (Tierney and deMenocal, 2013) indicating an aridification in East Africa during the Holocene supported by g)  $\delta D$  from leaf waxes from Lake Tanganyika (Tierney et al., 2008). The gray box indicates a period of a more negative IOD-like mean state in the Indian Ocean.

## 6. Summary

We present a continuous multi-proxy based reconstruction of the Holocene hydrography in the tropical eastern Indian Ocean, an area sensitive to IOD variability. Depth of thermocline and thermocline temperature reconstructions show a gradual decrease towards the late Holocene that might represent a shift to a more positive IOD-like mean state. Results from an orbital-forced climate model support our interpretation of long-term variations of the IOD-like mean state in the Indian Ocean. The gradual shift from a more negative IOD-like mean state to a more positive IOD-like mean state coincides with a shift from a westerly-dominated wind regime to an easterly-dominated wind regime during the IOD season. Additional temperature and rainfall records from both sides of the tropical Indian Ocean realm less affected by the monsoon system are essential in order to better assess sign and spatial extent of climate change and their relationship to the IOD.

## Acknowledgments

We acknowledge Silvana Pape, Monika Segl and Birgit Meyer-Schack for technical assistance. CCSM3 simulations were performed on the SGI Altix supercomputer of the Norddeutscher Verbund für Hoch- und Höchstleistungsrechnen (HLRN). We are grateful to Jeroen Groeneveld, Andreas Lückge and Markus Kienast for helpful discussions. This study greatly benefited from three constructive reviews. This work was funded by the BMBF projects SUMATRA (03G0189A), CAFINDO (03F0645A) as part of the SPICE III cluster, and supported by the DFG-Research Center/Cluster of Excellence “The Ocean in the Earth System”.

## References

- Abram, N.J., Gagan, M.K., Cole, J.E., Hantoro, W.S., Mudelsee, M., 2008. Recent intensification of tropical climate variability in the Indian Ocean. *Nat. Geosci.* 1, 849–853.
- Abram, N.J., Gagan, M.K., Liu, Z., Hantoro, W.S., McCulloch, M.T., Suwargadi, B.W., 2007. Seasonal characteristics of the Indian Ocean Dipole during the Holocene epoch. *Nature* 445, 299–302.
- Abram, N.J., McGregor, H.V., Gagan, M.K., Hantoro, W.S., Suwargadi, B.W., 2009. Oscillations in the southern extent of the Indo-Pacific Warm Pool during the mid-Holocene. *Quat. Sci. Rev.* 28, 2794–2803.
- Abreu, J.A., Beer, J., Ferriz-Mas, A., McCracken, K.G., Steinhilber, F., 2012. Is there a planetary influence on solar activity? *Astron. Astrophys.* 548 <http://dx.doi.org/10.1051/0004-6361/201219997>.
- Aldrian, E., Susanto, R., 2003. Identification of three dominant rainfall regions within Indonesia and their relationship to sea surface temperature. *Int. J. Climatol.* 23, 1435–1452.
- Anand, P., Elderfield, H., Conte, M.H., 2003. Calibration of Mg/Ca thermometry in planktonic foraminifera from a sediment trap time series. *Paleoceanography* 18. <http://dx.doi.org/10.1029/2002PA000846>.
- Ashok, K., Guan, Z., Saji, N.H., Yamagata, T., 2004. Individual and combined influences of ENSO and the Indian Ocean Dipole on the Indian Summer Monsoon. *J. Clim.* 17, 3141–3155.
- Barker, S., Greaves, M., Elderfield, H., 2003. A study of cleaning procedures used for foraminiferal Mg/Ca paleothermometry. *Geochim. Geophys. Geosyst.* 4 <http://dx.doi.org/10.1029/2003GC000559>.
- Behera, S.K., Krishnan, R., Yamagata, T., 1999. Unusual ocean-atmosphere conditions in the tropical Indian Ocean during 1994. *Geophys. Res. Lett.* 26, 3001–3004.
- Behera, S.K., Luo, J.J., Masson, S., Rao, S.A., Sakuma, H., Yamagata, T., 2006. A CGCM Study on the Interaction between IOD and ENSO. *J. Clim.* 19, 1688–1705.
- Bond, G., Kromer, B., Beer, J., Muscheler, R., Evans, M.N., Showers, W., Hoffmann, S., Lotti-Bond, R., Hajdas, I., Bonani, G., 2001. Persistent solar influence on North Atlantic climate during the Holocene. *Science* 294. <http://dx.doi.org/10.1126/science.1065680>.
- Cai, W., Cowan, T., Sullivan, A., 2009. Recent unprecedented skewness towards positive Indian Ocean Dipole occurrences and its impact on Australian rainfall. *Geophys. Res. Lett.* 36 <http://dx.doi.org/10.1029/2009GL037604>.
- Cai, W., Zheng, X.-T., Weller, E., Collins, M., Cowan, T., Lengaigne, M., Yu, W., Yamagata, T., 2013. Projected response of the Indian Ocean Dipole to greenhouse warming. *Nat. Geosci.* 6, 999–1007.
- Carton, J.A., Giese, B.S., Grodsky, S.A., 2005. Sea level rise and the warming of the oceans in the SODA ocean reanalysis. *J. Geophys. Res.* 110 <http://dx.doi.org/10.1029/2004JC002817>.
- Collins, W.D., Bitz, C.M., Blackmon, M.L., Bonan, G.B., Bretherton, C.S., Carton, J.A., Chang, P., Doney, S.C., Hack, J.J., Henderson, T.B., Kiehl, J.T., Large, W.G., McKenna, D.S., Santer, B.D., Smith, R.D., 2006. The Community Climate System Model version 3 (CCSM3). *J. Clim.* 19, 2122–2143.
- Debret, M., Bout-Roumaizelles, V., Grousset, F., Desmet, M., McManus, J.F., Massei, N., Sebag, D., Petit, J.-R., Copard, Y., Trentesaux, A., 2007. The origin of the 1500-year climate cycles in Holocene North-Atlantic records. *Clim. Past* 3, 569–575.
- de Boer, E.J., Tjallingii, R., Vélez, M.I., Rijdsdijk, K.F., Vlug, A., Reichert, G.-J., Prendergast, A.L., de Louw, P.G.B., Florens, F.B.V., Baider, C., Hooghiemstra, H., 2014. Climate variability in the SW Indian Ocean from an 8000-yr long multi-proxy record in the Mauritian lowlands shows a middle to late Holocene shift from negative IOD-state to ENSO-state. *Quat. Sci. Rev.* 86, 175–189.
- Ding, R., Li, J., 2012. Influences of ENSO teleconnection on the persistence of sea surface temperature in the tropical Indian Ocean. *J. Clim.* 25, 8177–8195.
- Deshpande, A., Chowdary, J.S., Gnanaseelan, C., 2014. Role of thermocline–SST coupling in the evolution of IOD events and their regional impacts. *Clim. Dyn.* 43, 163–174.
- Du, Y., Qu, T., Meyers, G., 2008. Interannual variability of sea surface temperature off Java and Sumatra in a global GCM\*. *J. Clim.* 21, 2451–2465.
- Du, Y., Qu, T., Meyers, G., Masumoto, Y., Sasaki, H., 2005. Seasonal heat budget in the mixed layer of the southeastern tropical Indian Ocean in a high-resolution ocean general circulation model. *J. Geophys. Res. Oceans* 110. <http://dx.doi.org/10.1029/2004JC002845>.
- Fleitmann, D., Burns, S.J., Mudelsee, M., Neff, U., Kramers, J., Mangini, A., Matter, A., 2003. Holocene forcing of the Indian Monsoon recorded in a stalagmite from southern Oman. *Science* 300. <http://dx.doi.org/10.1126/science.1083130>.
- Fleitmann, D., Burns, S.J., Mangini, A., Mudelsee, M., Kramers, J., Villa, I., Neff, U., Al-Subbary, A.A., Buettner, A., Hippler, D., Matter, A., 2007. Holocene ITCZ and Indian monsoon dynamics recorded in stalagmites from Oman and Yemen (Socotra). *Quat. Sci. Rev.* 26, 170–188.
- Gadgil, S., Vinayachandran, P.N., Francis, P.A., Gadgil, S., 2004. Extremes of the Indian summer monsoon rainfall, ENSO and equatorial Indian Ocean oscillation. *Geophys. Res. Lett.* 31 <http://dx.doi.org/10.1029/2004GL019733>.
- Garcin, Y., Melnick, D., Strecker, M.R., Olago, D., Tiercelin, J.-J., 2012. East African mid-Holocene wet–dry transition recorded in palaeo-shorelines of Lake Turkana, northern Kenya Rift. *Earth Planet. Sci. Lett.* 331–332, 322–334.
- Griffiths, M.L., Drysdale, R.N., Gagan, M.K., Zhao, J.-x., Ayliffe, L.K., Hellstrom, J.C., Hantoro, W.S., Frisia, S., Feng, Y.-x., Cartwright, I., Pierre, E. St., Fischer, M.J., Suwargadi, B.W., 2009. Increasing Australian-Indonesian monsoon rainfall linked to early Holocene sea-level rise. *Nat. Geosci.* 2, 636–639.
- Guan, Z., Yamagata, T., 2003. The unusual summer of 1994 in East Asia: IOD teleconnections. *Geophys. Res. Lett.* 30 <http://dx.doi.org/10.1029/2002GL016831>.
- Ihara, C., Kushnir, Y., Cane, M.A., 2008. Warming trend of the Indian Ocean SST and Indian Ocean Dipole from 1880 to 2004\*. *J. Clim.* 21, 2035–2046.
- Kuhnert, H., Kuhlmann, H., Mohtadi, M., Meggers, H., Baumann, K.-H., Pätzold, J., 2014. Holocene tropical western Indian Ocean sea surface temperatures in covariation with climatic changes in the Indonesian region. *Paleoceanography* 29. <http://dx.doi.org/10.1002/2013PA002555>.
- Li, T., Wang, B., Chang, C.P., Zhang, Y., 2003. A theory for the Indian Ocean Dipole–zonal mode\*. *J. Atmos. Sci.* 60, 2119–2135.
- Lorenz, S., Lohmann, G., 2004. Acceleration technique for Milankovitch type forcing in a coupled atmosphere–ocean circulation model: method and application for the Holocene. *Clim. Dyn.* 23, 727–743.
- Mohtadi, M., Max, L., Hebbeln, D., Baumgart, A., Krück, N., Jennerjahn, T., 2007. Modern environmental conditions recorded in surface sediment samples off W and SW Indonesia: planktonic foraminifera and biogenic compounds analyses. *Mar. Micropaleontol.* 65, 96–112.
- Mohtadi, M., Oppo, D.W., Lückge, A., DePol-Holz, R., Steinke, S., Groeneveld, J., Hemme, N., Hebbeln, D., 2011a. Reconstructing the thermal structure of the upper ocean: insights from planktic foraminifera shell chemistry and alkenones in modern sediments of the tropical eastern Indian Ocean. *Paleoceanography* 26. <http://dx.doi.org/10.1029/2011PA002132>.
- Mohtadi, M., Oppo, D.W., Steinke, S., Stuut, J.-B.W., De Pol-Holz, R., Hebbeln, D., Lückge, A., 2011b. Glacial to Holocene swings of the Australian-Indonesian monsoon. *Nat. Geosci.* 4, 540–544.
- Mohtadi, M., Prange, M., Oppo, D.W., De Pol-Holz, R., Merkel, U., Zhang, X., Steinke, S., Lückge, A., 2014. North Atlantic forcing of tropical Indian Ocean climate. *Nature*. <http://dx.doi.org/10.1038/nature13196>.
- Mohtadi, M., Steinke, S., Lückge, A., Groeneveld, J., Hathorne, E.C., 2010. Glacial to Holocene surface hydrography of the tropical eastern Indian Ocean. *Earth Planet. Sci. Lett.* 292, 89–97.
- Murtugudde, R., McCreary, J.P., Busalacchi, A.J., 2000. Oceanic processes associated with anomalous events in the Indian Ocean with relevance to 1997–1998. *J. Geophys. Res. Oceans* 105, 3295–3306.
- Naidu, C.V., Durgalakshmi, K., Muni Krishna, K., Ramalingeswara Rao, S., Satyanarayana, G.C., Lakshminarayana, P., Malleswara Rao, L., 2009. Is summer monsoon rainfall decreasing over India in the global warming era? *J. Geophys. Res. Atmos.* 114 <http://dx.doi.org/10.1029/2008JD011288>.
- Niedermeyer, E.M., Sessions, A.L., Feakins, S.J., Mohtadi, M., 2014. Hydroclimate of the western Indo-Pacific Warm Pool during the past 24,000 years. *PNAS* 111 (26), 9402–9406.
- Pena, L.D., Calvo, E., Cacho, I., Eggins, S., Pelejero, C., 2005. Identification and removal of Mn-Mg-rich contaminant phases on foraminiferal tests:

- implications for Mg/Ca past temperature reconstructions. *Geochem. Geophys. Geosyst.* 6 <http://dx.doi.org/10.1029/2005GC000930>.
- Ponton, C., Giosan, L., Eglinton, T.I., Fuller, D.Q., Johnson, J.E., Kumar, P., Collett, T.S., 2012. Holocene aridification of India. *Geophys. Res. Lett.* 39, L03704.
- Qiu, Y., Cai, W., Li, L., Guo, X., 2012. Argo profiles variability of barrier layer in the tropical Indian Ocean and its relationship with the Indian Ocean Dipole. *Geophys. Res. Lett.* 39 <http://dx.doi.org/10.1029/2012GL051441>.
- Qu, T., Meyers, G., 2005. Seasonal variation of barrier layer in the southeastern tropical Indian Ocean. *J. Geophys. Res. Oceans* 110. <http://dx.doi.org/10.1029/2004JC002816>.
- Saji, N.H., Goswami, B.N., Vinayachandran, P.N., Yamagata, T., 1999. A dipole mode in the tropical Indian Ocean. *Nature* 401, 360–363.
- Saji, N.H., Yamagata, T., 2003. Structure of SST and surface wind variability during Indian Ocean Dipole mode events: COADS observations\*. *J. Clim.* 16, 2735–2751.
- Spintall, J., Tomczak, M., 1992. Evidence of the barrier layer in the surface layer of the tropics. *J. Geophys. Res.* 97, 7305–7731.
- Steinke, S., Glatz, C., Mohtadi, M., Groeneveld, J., Li, Q., Jian, Z., 2011. Past dynamics of the East Asian monsoon: no inverse behaviour between the summer and winter monsoon during the Holocene. *Glob. Planet. Change* 78, 170–177.
- Swapna, P., Krishnan, R., 2008. Equatorial undercurrents associated with Indian Ocean Dipole events during contrasting summer monsoons. *Geophys. Res. Lett.* 35 <http://dx.doi.org/10.1029/2008GL033430>.
- Tierney, J.E., Smerdon, J.E., Anchukaitis, K.J., Seager, R., 2013. Multidecadal variability in East African hydroclimate controlled by the Indian Ocean. *Nature*. <http://dx.doi.org/10.1038/nature11785>.
- Tierney, J.E., deMenocal, P.B., 2013. Abrupt shifts in horn of Africa hydroclimate since the Last Glacial Maximum. *Science* 342, 843–846.
- Tierney, J.E., Russell, J.M., Huang, Y., Damsté, J.S.S., Hopmans, E.C., Cohen, A.S., 2008. Northern Hemisphere controls on tropical southeast African climate during the past 60,000 years. *Science* 322, 252–255.
- Varma, V., Prange, M., Merkel, U., Kleinen, T., Lohmann, G., Pfeiffer, M., Renssen, H., Wagner, A., Wagner, S., Schulz, M., 2012. Holocene evolution of the Southern Hemisphere westerly winds in transient simulations with global climate models. *Clim. Past* 8. <http://dx.doi.org/10.5194/cp-8-391-2012>.
- von Storch, H., Zwiers, F.W., 2004. *Statistical Analysis in Climate Research*. Cambridge University Press.
- Wang, Y., Cheng, H., Edwards, R.L., He, Y., Kong, X., An, Z., Wu, J., Kelly, M.J., Dykoski, C.A., Li, X., 2005. The Holocene Asian Monsoon: links to solar changes and North Atlantic climate. *Science* 308, 854–857.
- Webster, P.J., Moore, A.M., Loschnigg, J.P., Leben, R.R., 1999. Coupled ocean-atmosphere dynamics in the Indian Ocean during 1997–98. *Nature* 401, 356–360.
- Wiedicke-Hombach, M., et al., 2007. SUMATRA - the Hydrocarbon System of the Sumatra Forearc. Federal Institute for Geosciences and Natural Resources (BGR), Hannover. Vol. Archive No. 0126492.
- Yeager, S.G., Shields, C.A., Large, W.G., Hack, J.J., 2006. The low-resolution CCSM3. *J. Clim.* 19, 2545–2566.
- Yu, W., Xiang, B., Liu, L., Liu, N., 2005. Understanding the origins of interannual thermocline variations in the tropical Indian Ocean. *Geophys. Res. Lett.* 32 <http://dx.doi.org/10.1029/2005GL024327>.
- Zhao, Y., Nigam, S., 2015. The Indian Ocean Dipole: a monopole in SST. *Journal of Climate* 28. <http://dx.doi.org/10.1175/JCLI-D-14-00047.1>.